HHS Public Access

Author manuscript

Nat Immunol. Author manuscript; available in PMC 2014 September 01.

Published in final edited form as:

Nat Immunol. 2014 March ; 15(3): 231–238. doi:10.1038/ni.2810.

K63-linked polyubiquitylation of IRF1 transcription factor is essential for IL-1-induced CCL5 and CXCL10 chemokine production

Kuzhuvelil B. Harikumar[#], **Jessie W. Yester**[#], **Michael J. Surace**[#], **Clement Oyeniran**[#], **Megan M. Price**[#], **Wei-Ching Huang**[#], **Nitai C. Hait**[#], **Jeremy C. Allegood**[#], **Akimitsu Yamada**[#,±], **Xiangqian Kong**[$], **Helen M. Lazear**[§], **Reetika Bhardwaj**[#], **Kazuaki Takabe**[#,±], **Michael S. Diamond**[§], **Cheng Luo**[$], **Sheldon Milstien**[#], **Sarah Spiegel**[#], and **Tomasz Kordula**[#,*]

[#]Department of Biochemistry and Molecular Biology, the Massey Cancer Center, Virginia Commonwealth University School of Medicine, Richmond, VA 23298, USA

[±]Department of Surgery, and the Massey Cancer Center, Virginia Commonwealth University School of Medicine, Richmond, VA 23298, USA

[$]State Key Laboratory of Drug Research, Shanghai Institute of Materia Medica, Chinese Academy of Sciences, Shanghai 201203, China

[§]Departments of Medicine, Molecular Microbiology, Pathology & Immunology, Washington University School of Medicine, St. Louis, MO 63110, USA.

Abstract

Although interleukin-1 (IL-1) induces expression of interferon regulatory factor 1 (IRF1), its roles in immune and inflammatory responses and mechanisms of activation remain elusive. Here, we show that IRF1 is essential for IL-1-induced expression of chemokines CXCL10 and CCL5 that recruit mononuclear cells into sites of sterile inflammation. Newly synthesized IRF1 acquires K63-linked polyubiquitylation mediated by cellular inhibitor of apoptosis 2 (cIAP2), which is enhanced by the bioactive lipid sphingosine-1 phosphate (S1P). In response to IL-1, cIAP2 and sphingosine kinase 1, the enzyme that generates S1P, form a complex with IRF1, which leads to its activation. Thus, IL-1 triggers a hitherto unknown signaling cascade that controls induction of IRF1-dependent genes important for sterile inflammation.

IL-1 is a pleiotropic cytokine that regulates a broad range of both immune and inflammatory responses and plays a pivotal role in autoinflammatory diseases[1] but does not possess direct antiviral activity[2]. Accordingly, IL-1 induces expression of a variety of proinflammatory

[*]Address correspondence to: Dr. Tomasz Kordula, Department of Biochemistry and Molecular Biology, Virginia Commonwealth University, Richmond, Virginia 23298, tel. (804) 828-0771, fax. (804) 828-1473, tkordula@vcu.edu.

AUTHOR CONTRIBUTIONS

K.B.H. planned and performed experiments, with assistance from J.W.Y., M.S., C.O., M.M.P., N.C.H., J.C.A., A.Y., H.M.L., K.T., R.B., and M.S.D. X.K. and C.L. performed molecular docking. S.M., S.S. and T.K. conceived the study and contributed to planning of the experiments. T.K. wrote the initial draft of the manuscript, which was subsequently edited by all other authors.

cytokines and chemokines but does not stimulate production of significant amounts of type I interferons necessary to orchestrate antiviral responses. The inflammatory effects of IL-1 are mediated mainly by the activation of the transcription factor NF-κB and mitogen activated protein kinases (MAPKs)[3]. IL-1 initiates signaling upon binding to the IL-1 receptor (IL-1R) complex, containing IL-1R accessory protein that leads to the recruitment of the cytosolic adaptor protein MyD88 via the Toll-IL-1R domain of IL-1R[4]. MyD88 recruits IL-1R-associated kinase 4 (IRAK4) and IRAK1 resulting in hyperphosphorylation of IRAK1 by IRAK4[5]. Tumor necrosis factor (TNF) receptor-associated factor 6 (TRAF6), an E3 ubiquitin ligase containing a RING domain, is then recruited and activated[6]. TRAF6 conjugates K63-linked polyubiquitylation chains to itself and to IRAK1, which allows for the recruitment of the transforming growth factor β-activated kinase 1 (TAK1), TAK1-binding protein 2 (TAB2), TAB3, and the linear ubiquitin assembly (LUBAC) complex. In turn, LUBAC generates linear-polyubiquitin chains that recruit inhibitor of NF-κB kinase (IKK) complex[7]. Subsequently, TRAF6 decorates both IKKγ, a regulatory subunit of the IKK complex, and TAK1 with K63-linked polyubiquitin chains leading to the activation of NF-κB and MAPKs[8-11]. In addition to this activation cascade that requires the RING domain of TRAF6, NF-κB can also be activated by the oligomerization of MAPK kinase kinase 3, which is orchestrated by TRAF6 and requires its zinc finger domain but not a functional RING domain[12].

While Toll-like receptor (TLR) ligands and IL-1 both activate NF-κB and MAPKs, which are required for antiviral and inflammatory responses, the antiviral response is restricted to TLRs due to their ability to induce production of type I interferon by activation of interferon regulatory factors (IRFs)[13]. IRF3 and IRF7 are critical regulators of type I interferon production; nevertheless, both IRF1 and IRF5 also can induce type I interferons in TLR- and cell-specific manners[14,15]. Although *Irf1*$^{-/-}$ mice show normal serum concentrations of type I interferons[16], IRF1 regulates TLR9-induced interferon-β (IFN-β) production in conventional dendritic cells[14], expression of low amounts of IFN-β induced by TNF[17], expression of nitric oxide synthase and p35 subunit of IL-12 in macrophages[18], and priming of chromatin in interferon-β (IFN-β) stimulated macrophages[19]. IRF1 also controls recruitment of macrophages by TNF-activated endothelial cells[20], immune responses to West Nile virus infections[21], and pathogenesis of autoimmune diseases[22], including collagen-induced arthritis and experimental autoimmune encephalomyelitis (EAE) in mice.

Although expression of several IRFs is induced by both interferons and cytokines, activation of these IRFs requires acquisition of posttranscriptional modifications, including K63-linked polyubiquitylation and phosphorylation. TRAF6 serves as an E3 ubiquitin ligase for both IRF5[15] and IRF7[23] and K63-linked polyubiquitylation of IRF7 is a prerequisite for subsequent phosphorylation[23]. Expression of IRF1 is strongly induced by IFNβ and it can be further activated by TLRs[24]. The mechanism of this activation is not known, but it involves formation of a complex of IRF1 with MyD88[24]. IL-1 also induces expression of IRF1 and MyD88 is an adaptor for IL-1 signaling.

In this study, we show that IRF1 controls expression of delayed IL-1 responsive genes, particularly those encoding chemokines CXCL10 and CCL5, which are important for the recruitment of mononuclear cells into sites of sterile inflammation. In response to IL-1,

newly synthesized IRF1 is K63-linked polyubiquitylated by cellular inhibitor of apoptosis 2 (cIAP2), which requires the bioactive sphingolipid mediator sphingosine-1-phosphate (S1P) that directly binds to and enhances its E3 ubiquitin ligase activity. Thus, in addition to well-documented NF-κB-activation pathways, IL-1 triggers a hitherto undefined signaling pathway that regulates a set of IRF1-responsive genes important for sterile inflammation.

RESULTS

IL-1 induces CXCL10 and CCL5 expression via IRF1

IL-1 orchestrates immune and inflammatory responses by regulating expression of its target genes in multiple cell types by several molecular mechanisms. In human astrocytes, as previously reported for other cell types, IL-1 rapidly induced expression of genes controlled by the activation of NF-κB and MAPKs, including those encoding IL-6, IL-8, and CCL4 (**Supplementary Fig. 1a**). In addition, in both human and mouse astrocytes, IL-1 induced mRNA expression of chemokines CXCL10 and CCL5 (**Fig. 1a, b, Supplementary Fig. 1b**), whose promoters contain ISRE elements that can either bind IRFs or the ISGF3 complex (STAT1-STAT2-IRF9)[17,25]. IL-1 rapidly induced expression of IRF1 mRNA (**Fig. 1a-c**), accumulation of IRF1 protein, and its subsequent accumulation in the nucleus (**Fig. 1a**). Deletion of IRF1 in mouse embryonic fibroblasts (MEFs) almost completely eliminated the induction of CXCL10 and CCL5 mRNA by IL-1 observed in wild-type MEFs, whereas IL-6 mRNA expression was decreased to a lesser extent (**Fig. 1c**). We next examined whether IRF1 deficiency also impaired production of these chemokines *in vivo*. Intraperitoneal administration of IL-1 to wild-type mice resulted in dramatic increases of CXCL10 and CCL5 levels in the serum, while these responses to IL-1 were almost completely ablated in *Irf1*$^{-/-}$ mice (**Fig. 1d**). In contrast to CXCL10 and CCL5, IL-1-induced IL-6 expression was similar in wild-type and *Irf1*$^{-/-}$ mice (**Fig. 1d**). The specific requirement for IRF1 was further examined *in vivo* using *Stat1*$^{-/-}$ and *Irf3*$^{-/-}$*Irf7*$^{-/-}$ double-knockout mice. Although IRF3 and IRF7 regulate expression of CXCL10 and CCL5 upon TLR activation[26,27], and their expression also can be induced by the STAT1/STAT2/IRF9 heterotrimer[17,25], CXCL10 and CCL5 concentration in the serum of IL-1-treated *Irf3*$^{-/-}$*Irf7*$^{-/-}$ and *Stat1*$^{-/-}$ knockout mice were similar to wild-type mice (**Fig. 1e**). Thus, IRF1, but not IRF3 and IRF7, is essential for IL-1-induced expression of CXCL10 and CCL5 in cells and *in vivo*.

IRF1 regulates the recruitment of mononuclear cells

Since a deficiency of IRF1 results in autoimmune diseases[22] that are thought to be caused by dysfunction of T cells[28], the importance of IRF1 activation was examined further using the turpentine model of irritant-induced sterile inflammation that is IL-1-dependent[29]. Expression of CXCL10 and CCL5 mRNA was strongly induced at the sites of turpentine injection in wild-type mice but substantially reduced in *Irf1*$^{-/-}$ animals (by 92% and 97%, respectively) (**Fig. 2a**). Expression of IRF1-independent cytokine mRNAs coding for CCL2, IL-1, and IL-6, was also affected in *Irf1*$^{-/-}$ animals but to a lesser extent (by 48%, 78%, and 79%, respectively) (**Fig. 2a**). Although subsequent infiltration of inflammatory cells into the irritated skin area was evident in both wild-type and *Irf1*$^{-/-}$ mice (**Fig. 2b**), the infiltration of CD8^{+} T cells was attenuated in *Irf1*$^{-/-}$ animals. There was also a trend suggesting that infiltration of CD4^{+} T cells, monocytes (CD11b^{+}Gr-1^{-}), and bone marrow-derived immature

myeloid cells ($CD11b^+Gr\text{-}1^+$) was attenuated in *Irf1*$^{-/-}$ animals (**Fig. 2c, Supplementary Fig. 2a-c**). The diminished infiltration of these cells likely was a result of lower local expression of CXCL10 and CCL5 in *Irf1*$^{-/-}$ mice (**Fig. 2a**), and not the difference in the initial numbers of immune cells subsets. Although numbers of $CD8^+$ cells are much lower in *Irf1*$^{-/-}$ mice[30], the numbers of $CD4^+$ cells, monocytes and bone marrow-derived immature myeloid cells are comparable in *Irf1*$^{-/-}$ and WT animals (**Supplementary Fig. 2d**). Collectively, these data suggest that IRF1-dependent CXCL10 and CCL5 expression is required for the effective recruitment of mononuclear cells into sites of sterile inflammation.

IL-1 induces K63-linked polyubiquitylation of IRF1

IRF3 is phosphorylated by the IKKε-TBK-1 complex[31], whereas IRF1 requires IKKα for its activation by TLR9[14]. In addition to phosphorylation, IRF3, IRF5, and IRF7 undergo K63-linked polyubiquitylation that is needed for their activation[15,23,32] and this modification is a prerequisite for IRF7 phosphorylation[23]. To examine whether activation of IRF1 by IL-1 also involves its K63-linked polyubiquitylation, HEK293 cells co-expressing IRF1 and either wild-type-, K63-only-, or K48-only ubiquitin were stimulated with IL-1. Indeed, IL-1 enhanced K63-linked polyubiquitylation of IRF1, whereas K48-linked polyubiquitylation that targets IRF1 for degradation was not affected (**Fig. 3a**). IL-1-induced K63-linked polyubiquitylation of IRF1 also was detected using specific anti-K63-ubiquitin antibodies (**Fig. 3b**). In searching for the E3 ubiquitin ligase that mediates IL-1-induced K63-linked polyubiquitylation of IRF1, we focused on TRAF6, which is indispensable for IL-1-induced NF-κB activation[6]. We also tested cIAP1 and cIAP2 because expression of these E3 ligases is induced by NF-κB[33], which is activated by IL-1. S1P was included in the *in vitro* ubiquitylation reactions since S1P is a cofactor for E3 ligase activity of TRAF2 that mediates K63-linked polyubiquitylation of receptor interacting protein 1 (RIP1) in response to TNF signaling[34]. Although incubation of IRF1 with ubiquitin, the ubiquitin-activating enzymes E1, E2 Ubc5a, and either TRAF2, TRAF6, or cIAP1 failed to produce polyubiquitylated IRF1 *in vitro*, cIAP2 effectively polyubiquitylated IRF1 in the presence of S1P (**Fig. 3c**). Moreover, S1P enhanced both total and K63-linked polyubiquitylation but had no effect on the K48-linked polyubiquitylation of IRF1 (**Fig. 3d**). Furthermore, the stimulatory effect of S1P was specific, as other structurally related phospholipids, including dihydro-S1P, sphingosine, dihydro-sphingosine and lysophosphatidic acid were ineffective at inducing K63-linked polyubiquitylation of IRF1 (**Fig. 3e**). Polyubiquitylation of IRF1 was also evident in TNF-treated cells (**Fig. 3f**), which correlates with the previously described activation of IRF1 by TNF[17].

To identify sites of polyubiquitylation, we generated IRF1 lysine to arginine mutants (**Fig. 3g**), and tested for their ability to induce an IFN-β reporter gene. We found that wild-type IRF1 and IRF1 mutants (m1, m2, and m3), containing Lys 75, 78, 95, and 101, efficiently activated the reporter, which was enhanced by IL-1 (**Fig. 3h**). The wild-type IRF1 and the m3 mutant (containing Lys 75, 78, 95, and 101 only) were also K63 polyubiquitylated (**Fig. 3i**) and their polyubiquitylation was enhanced by IL-1. In contrast, an m4 IRF1 mutant lacking these lysines was not K63 polyubiquitylated and did not activate the reporter, suggesting that at least one of lysines (75, 78, 95, or 101) is a site of polyubiquitylation and is important for IRF1 function. IL-1 also efficiently promoted ubiquitylation of cIAP2 (**Fig.**

3j, k), suggesting cIAP2 activation. Together, these results suggest that activation of IRF1 requires K63-linked polyubiquitylation, and this is mediated by cIAP2 in the presence of S1P.

IL-1 induces formation of TRAF6-cIAP2-SphK1-IRF1 complex

cIAP2 and S1P have not been implicated previously in IL-1-induced signaling or activation of IRFs by IL-1R or TLRs. For that reason, it was important to demonstrate that cIAP2 and SphK1, one of the two isoenzymes capable of producing S1P, can be recruited to the known IL-1-induced signaling complexes. Stimulation with IL-1 induced sustained phosphorylation of SphK1 on Ser225 (**Fig. 4a**), which is known to enhance its enzymatic activity[35]. Accordingly, the amount of S1P doubled 2 hours after IL-1 stimulation of astrocytes (**Fig. 4b**), suggesting that S1P is produced at the time of activation of newly synthesized IRF1 (**Fig. 1a**). We also could coimmunoprecipitate SphK1 and cIAP2 and this interaction was enhanced by IL-1 (**Fig. 4c, d**), indicating that S1P produced by SphK1 is available to bind to cIAP2. Moreover, IL-1 enhanced the interaction of endogenous cIAP2 with SphK1 (**Fig. 4e**). To understand mechanistic basis of cIAP2 activation by IL-1 signaling, we first examined whether IL-1-activated TRAF6 recruits cIAP2. IL-1 promoted interaction of TRAF6 and cIAP2 (**Fig. 4f, g, h**), which contrasts previously reported constitutive interaction of cIAP2 with TRAF2 (**Fig. 4g** and[36]), and suggests that cIAP2 is specifically recruited by IL-1-activated TRAF6. Thus, IL-1-induced activation of TRAF6 leads to the recruitment of both cIAP2 and SphK1, and phosphorylation of SphK1, which can locally produce S1P. Moreover, IL-1 also stimulated the interaction of cIAP2 with IRF1 (**Fig. 4i**), suggesting that IRF1 also is recruited to this complex. These data suggest that IL-1 signaling recruits both SphK1 and cIAP2, which may be important for IRF1 activation.

SphK1 is needed for IL-1-induced chemokine expression

Since S1P was required for cIAP2-mediated K63-linked polyubiquitylation of IRF1 *in vitro* (**Fig. 3c**) and SphK1 associated with cIAP2 (**Fig. 4c-e**), it was important to test whether SphK1 is indispensable for IL-1-induced CXCL10 and CCL5 expression *in vitro* and *in vivo*. SKI-1, a highly specific small molecule SphK1 inhibitor[37], abolished IL-1-induced CCL5 mRNA expression and reduced IL-1-induced CXCL10 mRNA expression by 50% in primary human astrocytes (**Fig. 5a**). However, SKI-1 had no effect on the basal or IL-1-induced expression of IRF1 or SphK1 mRNAs, suggesting that SphK1 activity is needed specifically for IL-1-induced expression of IRF1-dependent genes. SKI-1 also strongly decreased concentrations of CXCL10 and CCL5 in the serum of mice administered exogenous IL-1 (**Fig. 5b**) but had no effect on the concentration of IL-6, whose expression is not regulated by IRF1. Thus, pharmacological inhibition of SphK1 specifically inhibits IL-1-induced expression of IRF1-dependent genes *in vitro* and *in vivo*. We also tested whether IL-1-induced expression of CXCL10 and CCL5 was altered in *Sphk1*$^{-/-}$ mice. Although SphK1 deficiency results in elevated basal mRNA expression of both IRF1-dependent and IRF1-independent cytokines, it also reduced IL-1-induced mRNA expression of CXCL10 and CCL5 but not IL-6 (**Fig. 5c**). Thus, SphK1 and its enzymatic activity are critical for the IL-1-induced expression of CCL5 and CXCL10.

cIAP2 is needed for IL-1-induced chemokine expression

In vitro ubiquitylation data suggested that cIAP2 but not cIAP1 mediates K63-linked polyubiquitylation of IRF1 in the presence of S1P (**Fig. 3c**). Accordingly, IL-1-induced expression of CCL5 mRNA was completely abolished in MEFs lacking cIAP2 (*Birc3*$^{-/-}$ MEFs) and expression of CXCL10 mRNA was profoundly diminished (**Fig. 6a**). In contrast, IL-1-induced expression of NF-κB-dependent genes, including IRF1, CCL2, and CXCL9 was normal in *Birc3*$^{-/-}$ MEFs (**Fig. 6a**), supporting previous reports that cIAP1 and cIAP2 are redundant for many biological functions, including their role in NF-κB activation[38] . To test if cIAP2 is needed for IL-1-induced polyubiquitylation of IRF1, cells were pretreated with Smac mimetic (SMAC), which causes degradation of both cIAP1 and cIAP2[39]. SMAC effectively blocked both basal and IL-1-induced polyubiquitylation of IRF1 (**Fig. 6b**). To confirm that cIAP2 mediates IRF1 polyubiquitylation, IRF1 ubiquitylation was analyzed in wild-type and *Birc3*$^{-/-}$ MEFs. Although IL-1 induced effective polyubiquitylation of IRF1 in wild-type MEFs, it failed to induce significant IRF1 polyubiquitylation in *Birc3*$^{-/-}$ MEFs (**Fig. 6c**). These data suggest that cIAP2 but not cIAP1 mediates polyubiquitylation of IRF1, which activates IRF1 and its downstream gene expression.

S1P binds to cIAP2 and promotes IRF1 polyubiquitylation

Previous studies have shown that S1P binds to TRAF2 and promotes K63-linked polyubiquitylation of RIP1 in response to TNF[34]. To assess whether S1P promotes polyubiquitylation of IRF1 by binding to cIAP2, both IRF1 and cIAP2 were immunoprecipitated and binding of S1P was analyzed by liquid chromatography electrospray ionization mass spectrometry (LC-ESI-MS/MS). S1P clearly bound to cIAP2 but not to IRF1 (**Fig. 7a**), suggesting that S1P binds to cIAP2. In agreement, ^{32}P-labeled-S1P effectively bound to recombinant cIAP2, and this binding competed with unlabeled S1P but not by other related lipids, including sphingosine and lysophosphatidic acid (**Fig. 7b**). Molecular modeling of S1P binding into cIAP2 suggested that S1P binds to the groove present in the RING domain of cIAP2 (**Fig. 7c**), and its binding could be stabilized further by a positively charged region (containing Thr594 and Lys596) interacting with the phosphate group of S1P (**Supplementary Fig. 3a**). To test these predictions, a cIAP2 mutant [cIAP2(AAA)] containing Thr594Ala, Ile595Ala, and Lys596Ala, was generated and tested for S1P binding and *in vitro* E3 ligase activity using IRF1 as a substrate. As a negative control, a cIAP2 RING domain point mutant (His574Ala) that does not contain E3 ligase activity[40] was used. Binding of S1P to the cIAP2(H574A) mutant was markedly diminished (**Fig. 7d**) and this mutant no longer polyubiquitylated IRF1 (**Fig. 7e**). In agreement with the molecular modeling data (**Fig. 7c, Supplementary Fig. 3**) and in contrast to wild-type cIAP2, the cIAP2(AAA) mutant failed to bind S1P efficiently (**Fig. 7d**) and lost its *in vitro* E3 ligase activity towards IRF1 (**Fig. 7e**).

Collectively, our studies uncovered a hitherto undescribed signaling cascade activated by IL-1 (**Supplementary Fig. 4**) that leads to the activation of newly synthesized IRF1 and subsequent induction of IRF1-dependent genes. Activation of IRF1 requires its K63-linked polyubiquitylation mediated by cIAP2 and depends on the production of S1P by SphK1.

DISCUSSION

In comparison to IRF3 and IRF7, considerably less is known about IRF1 function and regulation. In addition to previously known functions, TNF-activated IRF1 induces expression of several chemokines and low levels of IFNβ that subsequently activate the ISGF3 complex and sustain expression of TNF-induced chemokines[17]. It has also been demonstrated that recruitment of monocytes by endothelial cells requires activation of IRF1 by TNF receptor 2[20]. Here, we demonstrate that IRF1 also is required for IL-1-induced expression of CXCL10 and CCL5 in astrocytes and MEFs *in vitro* and in mice *in vivo*. Furthermore, IRF1 is required for turpentine-induced, IL-1-dependent expression of CXCL10 and CCL5 and subsequent recruitment of mononuclear cells into sites of sterile inflammation. The importance of local chemokine production is further supported by findings that *Irf1*$^{-/-}$ mice with wild-type bone marrow present milder EAE clinical signs and shorter disease duration compared to wild-type mice[41]. Therefore, our findings may in part explain the diminished susceptibility of *Irf1*$^{-/-}$ mice to autoimmune diseases, such as collagen-induced arthritis and EAE that are in part IL-1-dependent.

Transcriptional induction of IRF1 and stabilization of IRF1 protein are likely not sufficient for activation of IRF1-dependent genes. IFN-γ-induced expression of CXCL10 requires further activation of IRF1, possibly by phosphorylation[25]. Indeed, IKKβ is needed for IRF1-dependent expression of CXCL10 in response to IFN-γ[25] whereas activation of IRF1 following TLR7 and TLR9 signaling requires IKKα, which coimmunoprecipitates with IRF1 and phosphorylates IRF1 *in vitro*[14]. Analogously, other IRFs are activated via phosphorylation, with IRF7 phosphorylation requiring prior K63-linked polyubiquitylation by TRAF6[23]. Although IRF1 stability is controlled by its K48-linked polyubiquitylation that targets it for proteasomal degradation[42], we now present evidence that IRF1 also undergoes K63-linked polyubiquitylation in response to IL-1. K63-linked polyubiquitylation of IRF1 occurs in its DNA binding domain and thus may counteract constitutive K48-linked polyubiquitylation, which also targets residues in the DNA binding domain of IRF1[42]. IFN-γ-induced IRF1 is known to form a complex with, and is activated by, MyD88 upon TLR stimulation by a process referred to as 'MyD88-dependent licensing'[24]. Thus, our finding that activation of the IL-1R complex, which utilizes MyD88 as a signaling adaptor, leads to IRF1 K63-linked polyubiquitylation, suggests that MyD88-dependent licensing likely involves K63-linked polyubiquitylation. However, we found that TRAF6, an E3 ubiquitin ligase that orchestrates NF-κB and MAPK activation in response to IL-1[43], does not mediate polyubiquitylation of IRF1. In response to IL-1, cIAP2 is recruited to TRAF6 and becomes polyubiquitylated, which suggests cIAP2 activation. The closely related cIAP1 and cIAP2 are redundant for many of their known functions; nevertheless, they also have unique functions, such as cIAP1-coordinated activation of NF-κB in response to DNA damage[41]. K63-linked polyubiquitylation of IRF1 is unambiguously mediated by cIAP2 but not by cIAP1. Since IL-1-induced IRF1 polyubiquitylation and activation of IRF1-dependent genes is almost completely abrogated in *Birc3*$^{-/-}$ MEFs, cIAP2 likely plays critical and non-redundant role in the activation of IRF1-dependent responses. This is further supported by the findings that cIAP2 mutants that lack E3 ubiquitin ligase activity or S1P binding failed to polyubiquitylate IRF1 *in vitro*.

S1P also is required for K63-linked polyubiquitylation of IRF1 by cIAP2, highlighting another novel direct intracellular target for this signaling lipid. Recently, intracellular S1P has been shown to bind directly to several intracellular targets and specifically regulate their activity (reviewed in[44]). We detected efficient and specific binding of S1P to cIAP2. Furthermore, molecular modeling of S1P binding to cIAP2 identified potentially important amino acids and allowed for the generation of a cIAP2 mutant that neither binds S1P nor polyubiquitylates IRF1 *in vitro*, suggesting that S1P serves as a *bona fide* obligatory cofactor for E3 ligase activity of cIAP2. Since SphK1 is activated in response to IL-1 and also coimmunoprecipitates with cIAP2, S1P is likely generated at the time of cIAP2 activation. This mechanism is similar to the one observed after TNF stimulation where SphK1 is also activated and forms a complex with TRAF2[34]. The importance of SphK1 for IL-1-induced IRF1-dependent gene expression is supported further by our finding that pharmacological inhibition of SphK1 activity or genetic deletion of SphK1 diminishes expression of IRF1-dependent genes *in vitro* and *in vivo*.

Our data collectively suggest that in contrast to TLRs that efficiently recruit mononuclear immune cells to sites of infection by IRF3- and IRF7-dependent activation of chemokine expression, the recruitment of these immune cells to sites of sterile inflammation is coordinated by IL-1R-mediated activation of IRF1. Since IRF1 affects pathogenesis of autoimmune diseases[22], targeting of this hitherto unrecognized IL-1-induced cascade may be clinically important in the future.

METHODS

Mice

Irf1$^{-/-}$ mice were obtained from Jackson Laboratory (Bar Harbor, ME), *Sphk1*$^{-/-}$ mice were provided by Dr. Richard Proia, National Institutes of Health (Bethesda, MD), and *Stat1*$^{-/-}$ mice were provided by Dr. Andrew Larner, VCU (Richmond, VA). *Irf3*$^{-/-}$*Irf7*$^{-/-}$ double-knockout mice[46] were generated and housed at WUSM, while all other mice were housed at VCU according to guidelines of VCU Institutional Animal Care and Use Committee and mouse protocols were approved by the institutional IACUC. 8-16 week old male and female mice were used.

Turpentine-induced inflammation

A turpentine abscess was initiated under anesthesia by injection (50 μl, s.c.) of pure gum spirits of turpentine into age-matched males and females wild-type or *Irf1*$^{-/-}$ mice (littermates, 6-8 week old). Animals were sacrificed after 8h or 24h and skin and underlying muscles at the site of injection, containing was collected for mRNA analysis, flow cytometry, and staining.

Cell culture and transfections

HEK293 cells (ATCC, Manassas, VA) were cultured as described[34]. Mouse embryo fibroblasts were prepared from E13 embryos using standard protocols. Mouse astrocytes were kindly provided by Dr. Pamela Knapp (VCU, Richmond, VA). Human cortical astrocytes were prepared from fetal tissue provided by Advanced Bioscience Resources, Inc.

(Alameda, CA) and cultured as previously described[47]. Cells were stimulated with 10 ng/ml IL-1 for 2h, unless indicated otherwise. Cells were transfected with expression plasmids using either Lipofectamine Plus (Invitrogen) or TransIT2020 reagent (Mirus, Madison, WI).

Reagents, plasmids and antibodies

S1P, sphingosine, dihydroS1P, lysophosphatydic acid, and SK1-I ((2R,3S,4E)-N-methyl-5-(4'-pentylphenyl)-2-aminopent-4-ene-1,3-diol) were obtained from Enzo Life Sciences International (Farmingdale, NY). Ubiquitin conjugating enzymes, wild-type, K63-only, and K48-only ubiquitin were from Boston Biochem (Cambridge, MA). IL-1β, recombinant *E.coli*-derived cIAP1 and cIAP2, and anti-pan-cIAP1/2 were from R&D Systems (Minneapolis, MN). The following antibodies were used: anti-IRF1, anti-cIAP2, anti-ubiquitin, anti-TRAF6 (Santa Cruz Biotechnology, Santa Cruz, CA); anti-His-tag (27E8), anti-tubulin (Cell Signaling Technology, Danvers, MA); anti-SphK1 antibodies were described previously[48]; anti-phospho-SphK1(Ser225) (ECM Biosciences, Versailles, KY); anti-HA (Roche, Indianapolis, IN); anti-ubiquitin-K63 (HWA4C4) (eBiosciences, San Diego, CA); and anti-ubiquitin-K48 (Apu2) (Millipore, Billerica, MA), APC-anti-CD4 (100412), PE/Cy7-anti CD8a (100721), FITC-anti-CD45 (103107), PerCP/Cy5.5-anti-CD11b (101227), PE-anti-Ly-6G/Ly-6C (Gr1) (108408), and isotope matched control antibodies (BioLegend, San Diego, CA). HA-agarose beads, FLAG M2 affinity beads, anti-FLAG (M2) antibodies, FLAG and HA peptides were from Sigma-Aldrich (St. Louis, MO). Ni-NTA affinity beads were from Qiagen (Valencia, CA). SMAC mimetic was a gift of Dr. Xiaodong Wang (University of Texas-Southwestern, Dallas, TX). Expression plasmids coding for wild-type TRAF2, His-TRAF6, and HA-tagged ubiquitins were kindly provided by Dr. Bryant Darnay (MD Anderson, Houston, TX), Dr. Xiang-Yang Wang (VCU, Richmond, VA), and Dr. Zhijian Chen (University of Texas-Southwestern, Dallas, TX), respectively. The IFN-β reporter was provided by Dr. K.A. Fitzgerald (University of Massachusetts, Worcester, MA). Expression plasmid coding for HA-tagged cIAP2 and *Birc3*$^{-/-}$ MEFs were provided by Dr. Colin Duckett (University of Michigan, Ann Arbor, MI). Plasmid encoding mouse IRF1 was purchased from Open Biosystems (Lafayette, CO). Coding region of IRF1 was amplified by PCR and cloned into pCMV-FLAG5A (Sigma-Aldrich, St. Louis, MO). Lys to Arg mutants of IRF1 were generated by QuikChange Lightning Multi Site-Directed Mutagenesis Kit while cIAP2(AAA)-HA mutant was generated by QuikChange II site-directed mutagenesis kit (both from Agilent Technologies, Santa Clara, CA).

Immunofluorescence

Frozen sections (10 μm) were prepared from tissue embedded in optimal cutting medium (OCT 4583, Sakura Finetek, Torrance, CA). Sections were fixed in 4% paraformaldehyde, blocked with horse serum containing 2.5% fraction V BSA for 1h, and then stained with anti-F4/80 (AbD Serotec, Oxford, UK) or anti-CD90.2 (eBiosciences, San Diego, CA) antibodies at 4°C overnight. After three washes with PBS, sections were stained with Alexa fluor 594-conjugated antibodies (Invitrogen, Grand Island, NY) for 20 min. Nuclei were stained with Hoechst for 5 min. Sections were examined with TCS-SP2 AOBS Confocal Laser Scanning Microscope (Leica).

Immunoblotting and immunoprecipitation

Cell lysates were prepared in 20 mM HEPES pH 7.4 containing 150 mM NaCl, 10 mM β-glycerophosphate, 1.5 mM $MgCl_2$, 10 mM NaF, 2 mM dithiothreitol, 1 mM NaV_3O_4, 2 mM EGTA, 1 mM PMSF, 0.5% Triton X-100, 1:500 protease inhibitor cocktail (Sigma-Aldrich), and 1 mg/ml of N-ethylmaleimide. For immunoprecipitation, cell lysates (500 μg) were incubated with antibodies overnight at 4°C. Immunoprecipitated complexes were captured using protein A/G-plus agarose beads (Santa Cruz Biotechnology, Santa Cruz, CA). After extensive washing, samples were boiled in SDS-PAGE sample buffer, and analyzed by immunoblotting. In some cases, FLAG-tagged proteins were immunoprecipitated with FLAG-M2 affinity beads overnight at 4°C and bound proteins eluted with FLAG peptide and analyzed by immunoblotting.

In vitro ubiquitylation and protein purification

Ubiquitylation assays were performed as described earlier with slight modifications[34]. FLAG-tagged IRF1 was purified from transfected HEK293 cells either using anti-FLAG M2 affinity beads and eluted with FLAG peptide or in some cases with anti-FLAG antibody. Recombinant *E. coli* derived His-tagged cIAP1, His-tagged cIAP2, or HA-tagged cIAP2 purified from transfected HEK293 cells were used as the E3 ligases. Ubiquitylation assays were carried out at 35°C for 2h in 50 mM HEPES, pH 7.8, containing 5 mM $MgCl_2$, 4 mM ATP, 50 nM E1, 10 μg ubiquitin (wild type, K48-only or K63-only), 450 nM UbcH5/Uev1a, purified E3 ligases, and IRF1-FLAG bound to the M2 agarose beads in the absence or presence of various lipids. In some experiments, 2 μg recombinant cIAP2 were used. Reactions were stopped by boiling in SDS-PAGE sample buffer, proteins were resolved by SDS-PAGE, and analyzed by immunoblotting.

Quantification of lipids by mass spectrometry

Cell lysates (500 μg) were immunoprecipitated with anti-HA, anti-FLAG or control antibodies. Lipids were extracted, and sphingolipids quantified by LC-ESI-MS/MS (4000 QTRAP, Applied Biosystems, Carlsbad, CA) as described [49].

[^{32}P]S1P binding assays

Lysates (500 μg) of cells overexpressing HA-cIAPs or vector were incubated with 20 μl of pre-cleared anti-HA agarose beads (Sigma-Aldrich, St. Louis, MO) overnight at 4°C. The beads were then washed extensively and incubated with [^{32}P]S1P (0.1 nM, 6.8 μCi/pmol) in the presence or absence of unlabeled lipids in 150 μl 50 mM Tris (pH 7.5), 137 mM NaCl, 1 mM $MgCl_2$, 2.7 mM KCl, 15 mM NaF, 0.5 mM NaV_3O_4 for 60 min at 4°C as described previously[34]. Bound cIAPs were eluted with 50 μl HA peptide (200 ng/ml). Bound [^{32}P]S1P was quantified with a LS6500 scintillation counter (Beckman Coulter, Brea, CA).

Quantitative PCR

Total RNA was prepared with Trizol (Invitrogen, Grand Island, NY) and 1 μg RNA was reverse-transcribed using the High Capacity cDNA Archive kit (Applied Biosystems, Carlsbad, CA). mRNA levels were examined using pre-mixed primer-probe sets and TaqMan Universal PCR Master Mix (Applied Biosystems). The cDNAs were diluted 10-

fold (for the target genes) or 100-fold (for GAPDH), and amplified using the ABI 7900HT cycler. Gene expression levels were normalized to GAPDH, and presented as a fold induction with mean values ± s.d. or s.e.m as indicated.

Quantification of cytokine and chemokine levels in vivo

Age-matched wild-type, *Irf1*$^{-/-}$, *Irf3*$^{-/-}$*Irf7*$^{-/-}$, *Stat1*$^{-/-}$, or *Sphk1*$^{-/-}$ mice (6-8 week old) were administered (i.p) either IL-1 (40 μg/kg) or PBS. Animals were sacrificed after 2h and serum was collected for cytokine and chemokine analysis. Protein levels were determined by ELISA using kits for CXCL10, CCL5 (R&D Systems, Minneapolis, MN) and IL-6 (BD Biosciences, San Diego, CA) according to manufacturer's protocols.

Molecular modeling of cIAP2 with S1P

The molecular docking program AutoDock 4.2 was used for the automated molecular docking simulations[45]. Briefly, the PDBQT files were created for both ligands and cIAP2 with Gasteiger charge assigned, and AutoGrid algorithm was employed to precalculate the atomic affinity grid used in the docking simulation. Complexes were selected based on criteria of interacting energy combined with geometrical matching quality. The program LIGPLOT version 4.4.2[50] was used to dissect the detailed interactions between ligands and cIAP2. An interaction was counted as hydrophobic interaction if the distance of two hydrophobic atoms between ligand and the protein residue is less than 3.9 Å, and counted as a hydrogen bond if (i) it is between a listed donor and acceptor and (ii) the angles and distances formed by the atoms surrounding the hydrogen bond lie within the default criteria.

Statistical analysis

All experiments were repeated at least three times, except as indicated in figure legends, with consistent results. Samples were not excluded. Data are presented as means ± s.d. or s.e.m., as indicated. For mouse studies, 4-7 randomly chosen animals were used per experimental group. Most of the animal experiments were blinded, whereas the majority of in vitro experiments were not. Statistical analysis was performed using SPSS Statistics 21 software. One-way ANOVA comparisons were performed using a Bonferroni post-hoc test, with $P<0.05$ considered statistically significant. Additionally, independent sample student T-test also was used to analyze data.

Supplementary Material

Refer to Web version on PubMed Central for supplementary material.

ACKNOWLEDGEMENTS

We thank Drs. B. Darnay, X-Y. Wang, Z. Chen, and C. Duckett for expression plasmids, Dr. R. Proia for *Sphk1*$^{-/-}$ mice, Dr. A. Larner for *Stat1*$^{-/-}$ mice, Dr. K. Fitzgerald for the INF-β reporter gene, Dr. P. Knapp for mouse astrocytes, Dr. J. Almenara for tissue processing, sectioning and staining. This work was supported by grants from the National Institute of Health 1R01AI093718 (to T.K.), 5R37GM043880 and 1U19AI077435 (both to S.S.), in part by R01CA160688 (to K.T), as well as in part by the National Natural Science Foundation of China (91029704) to C.L. Microscopy was performed at the VCU's Microscopy Facility supported by NIH grant 5P30NS047463. The Lipidomics Developing Shared Resource and the Flow Cytometry Cores were supported in part by NIH grant P30CA16059 to the Massey Cancer Center.

REFERENCES

1. Dinarello CA. Immunological and inflammatory functions of the interleukin-1 family. Annu Rev Immunol. 2009; 27:519–550. [PubMed: 19302047]
2. O'Neill LA. The interleukin-1 receptor/Toll-like receptor superfamily: 10 years of progress. Immunol Rev. 2008; 226:10–18. [PubMed: 19161412]
3. Arend WP. The balance between IL-1 and IL-1Ra in disease. Cytokine Growth Factor Rev. 2002; 13:323–340. [PubMed: 12220547]
4. Janssens S, Beyaert R. A universal role for MyD88 in TLR/IL-1R-mediated signaling. Trends Biochem Sci. 2002; 27:474–482. [PubMed: 12217523]
5. Kim TW, et al. A critical role for IRAK4 kinase activity in Toll-like receptor-mediated innate immunity. J Exp Med. 2007; 204:1025–1036. [PubMed: 17470642]
6. Inoue J, Gohda J, Akiyama T. Characteristics and biological functions of TRAF6. Adv Exp Med Biol. 2007; 597:72–79. [PubMed: 17633018]
7. Emmerich CH, et al. Activation of the canonical IKK complex by K63/M1-linked hybrid ubiquitin chains. Proc Natl Acad Sci U S A. 2013; 110:15247–15252. [PubMed: 23986494]
8. Chen ZJ. Ubiquitin signalling in the NF-kappaB pathway. Nat Cell Biol. 2005; 7:758–765. [PubMed: 16056267]
9. Deng L, et al. Activation of the IkappaB kinase complex by TRAF6 requires a dimeric ubiquitin-conjugating enzyme complex and a unique polyubiquitin chain. Cell. 2000; 103:351–361. [PubMed: 11057907]
10. Conze DB, Wu CJ, Thomas JA, Landstrom A, Ashwell JD. Lys63-linked polyubiquitination of IRAK-1 is required for interleukin-1 receptor- and toll-like receptor-mediated NF-kappaB activation. Mol Cell Biol. 2008; 28:3538–3547. [PubMed: 18347055]
11. Wang C, et al. TAK1 is a ubiquitin-dependent kinase of MKK and IKK. Nature. 2001; 412:346–351. [PubMed: 11460167]
12. Yamazaki K, et al. Two mechanistically and temporally distinct NF-kappaB activation pathways in IL-1 signaling. Sci Signal. 2009; 2:ra66. [PubMed: 19843958]
13. Hiscott J. Convergence of the NF-kappaB and IRF pathways in the regulation of the innate antiviral response. Cytokine Growth Factor Rev. 2007; 18:483–490. [PubMed: 17706453]
14. Hoshino K, et al. Critical role of IkappaB Kinase alpha in TLR7/9-induced type I IFN production by conventional dendritic cells. J Immunol. 2010; 184:3341–3345. [PubMed: 20200270]
15. Balkhi MY, Fitzgerald KA, Pitha PM. Functional regulation of MyD88-activated interferon regulatory factor 5 by K63-linked polyubiquitination. Mol Cell Biol. 2008; 28:7296–7308. [PubMed: 18824541]
16. Reis LF, Ruffner H, Stark G, Aguet M, Weissmann C. Mice devoid of interferon regulatory factor 1 (IRF-1) show normal expression of type I interferon genes. Embo J. 1994; 13:4798–4806. [PubMed: 7957048]
17. Yarilina A, Park-Min KH, Antoniv T, Hu X, Ivashkiv LB. TNF activates an IRF1-dependent autocrine loop leading to sustained expression of chemokines and STAT1-dependent type I interferon-response genes. Nat Immunol. 2008; 9:378–387. [PubMed: 18345002]
18. Liu J, Guan X, Tamura T, Ozato K, Ma X. Synergistic activation of interleukin-12 p35 gene transcription by interferon regulatory factor-1 and interferon consensus sequence-binding protein. J Biol Chem. 2004; 279:55609–55617. [PubMed: 15489234]
19. Qiao Y, et al. Synergistic Activation of Inflammatory Cytokine Genes by Interferon- gamma-Induced Chromatin Remodeling and Toll-like Receptor Signaling. Immunity. 2013; 39:454–469. [PubMed: 24012417]
20. Venkatesh D, et al. Endothelial TNF Receptor 2 Induces IRF1 Transcription Factor- Dependent Interferon-beta Autocrine Signaling to Promote Monocyte Recruitment. Immunity. 2013; 38:1025–1037. [PubMed: 23623383]
21. Brien JD, et al. Interferon regulatory factor-1 (IRF-1) shapes both innate and CD8(+) T cell immune responses against West Nile virus infection. PLoS Pathog. 2011; 7:e1002230. [PubMed: 21909274]

22. Tada Y, Ho A, Matsuyama T, Mak TW. Reduced incidence and severity of antigen-induced autoimmune diseases in mice lacking interferon regulatory factor-1. J Exp Med. 1997; 185:231–238. [PubMed: 9016872]
23. Ning S, Campos AD, Darnay BG, Bentz GL, Pagano JS. TRAF6 and the three C-terminal lysine sites on IRF7 are required for its ubiquitination-mediated activation by the tumor necrosis factor receptor family member latent membrane protein 1. Mol Cell Biol. 2008; 28:6536–6546. [PubMed: 18710948]
24. Negishi H, et al. Evidence for licensing of IFN-gamma-induced IFN regulatory factor 1 transcription factor by MyD88 in Toll-like receptor-dependent gene induction program. Proc Natl Acad Sci U S A. 2006; 103:15136–15141. [PubMed: 17018642]
25. Shultz DB, Rani MR, Fuller JD, Ransohoff RM, Stark GR. Roles of IKK-beta, IRF1, and p65 in the activation of chemokine genes by interferon-gamma. J Interferon Cytokine Res. 2009; 29:817–824. [PubMed: 19929594]
26. Lin R, Heylbroeck C, Genin P, Pitha PM, Hiscott J. Essential role of interferon regulatory factor 3 in direct activation of RANTES chemokine transcription. Mol Cell Biol. 1999; 19:959–966. [PubMed: 9891032]
27. Kawai T, et al. Lipopolysaccharide stimulates the MyD88-independent pathway and results in activation of IFN-regulatory factor 3 and the expression of a subset of lipopolysaccharide-inducible genes. J Immunol. 2001; 167:5887–5894. [PubMed: 11698465]
28. Dinarello CA. Anti-inflammatory Agents: Present and Future. Cell. 2010; 140:935–950. [PubMed: 20303881]
29. Leon LR, Conn CA, Glaccum M, Kluger MJ. IL-1 type I receptor mediates acute phase response to turpentine, but not lipopolysaccharide, in mice. Am J Physiol. 1996; 271:R1668–1675. [PubMed: 8997368]
30. Penninger JM, et al. The interferon regulatory transcription factor IRF-1 controls positive and negative selection of CD8+ thymocytes. Immunity. 1997; 7:243–254. [PubMed: 9285409]
31. Fitzgerald KA, et al. IKKepsilon and TBK1 are essential components of the IRF3 signaling pathway. Nat Immunol. 2003; 4:491–496. [PubMed: 12692549]
32. Zeng W, Xu M, Liu S, Sun L, Chen ZJ. Key role of Ubc5 and lysine-63 polyubiquitination in viral activation of IRF3. Mol Cell. 2009; 36:315–325. [PubMed: 19854139]
33. Schoemaker MH, et al. Cytokine regulation of pro- and anti-apoptotic genes in rat hepatocytes: NF-kappaB-regulated inhibitor of apoptosis protein 2 (cIAP2) prevents apoptosis. J Hepatol. 2002; 36:742–750. [PubMed: 12044523]
34. Alvarez SE, et al. Sphingosine-1-phosphate is a missing cofactor for the E3 ubiquitin ligase TRAF2. Nature. 2010; 465:1084–1088. [PubMed: 20577214]
35. Pitson SM, et al. Activation of sphingosine kinase 1 by ERK1/2-mediated phosphorylation. Embo J. 2003; 22:5491–5500. [PubMed: 14532121]
36. Zheng C, Kabaleeswaran V, Wang Y, Cheng G, Wu H. Crystal structures of the TRAF2: cIAP2 and the TRAF1: TRAF2: cIAP2 complexes: affinity, specificity, and regulation. Mol Cell. 2010; 38:101–113. [PubMed: 20385093]
37. Paugh SW, et al. A selective sphingosine kinase 1 inhibitor integrates multiple molecular therapeutic targets in human leukemia. Blood. 2008; 112:1382–1391. [PubMed: 18511810]
38. Zarnegar BJ, et al. Noncanonical NF-kappaB activation requires coordinated assembly of a regulatory complex of the adaptors cIAP1, cIAP2, TRAF2 and TRAF3 and the kinase NIK. Nat Immunol. 2008; 9:1371–1378. [PubMed: 18997794]
39. Petersen SL, et al. Autocrine TNFalpha signaling renders human cancer cells susceptible to Smac-mimetic-induced apoptosis. Cancer Cell. 2007; 12:445–456. [PubMed: 17996648]
40. Csomos RA, Brady GF, Duckett CS. Enhanced cytoprotective effects of the inhibitor of apoptosis protein cellular IAP1 through stabilization with TRAF2. J Biol Chem. 2009; 284:20531–20539. [PubMed: 19506082]
41. Hinz M, et al. A cytoplasmic ATM-TRAF6-cIAP1 module links nuclear DNA damage signaling to ubiquitin-mediated NF-kappaB activation. Mol Cell. 2010; 40:63–74. [PubMed: 20932475]

42. Narayan V, Pion E, Landre V, Muller P, Ball KL. Docking-dependent ubiquitination of the interferon regulatory factor-1 tumor suppressor protein by the ubiquitin ligase CHIP. J Biol Chem. 2011; 286:607–619. [PubMed: 20947504]

43. Cao Z, Xiong J, Takeuchi M, Kurama T, Goeddel DV. TRAF6 is a signal transducer for interleukin-1. Nature. 1996; 383:443–446. [PubMed: 8837778]

44. Yester JW, Tizazu E, Harikumar KB, Kordula T. Extracellular and intracellular sphingosine-1-phosphate in cancer. Cancer Metastasis Rev. 2011; 30:577–597. [PubMed: 22002715]

45. Morris GM, et al. Automated docking using a Lamarckian genetic algorithm and an empirical binding free energy function. J Comput Chem. 1998; 19:1639–1662.

46. Daffis S, Suthar MS, Szretter KJ, Gale M Jr. Diamond MS. Induction of IFN-beta and the innate antiviral response in myeloid cells occurs through an IPS-1-dependent signal that does not require IRF-3 and IRF-7. PLoS Pathog. 2009; 5:e1000607. [PubMed: 19798431]

47. Kordula T, et al. Oncostatin M and the interleukin-6 and soluble interleukin-6 receptor complex regulate alpha1-antichymotrypsin expression in human cortical astrocytes. J Biol Chem. 1998; 273:4112–4118. [PubMed: 9461605]

48. Hait NC, et al. Role of sphingosine kinase 2 in cell migration toward epidermal growth factor. J Biol Chem. 2005; 280:29462–29469. [PubMed: 15951439]

49. Hait NC, et al. Regulation of histone acetylation in the nucleus by sphingosine-1-phosphate. Science. 2009; 325:1254–1257. [PubMed: 19729656]

50. Wallace AC, Laskowski RA, Thornton JM. LIGPLOT: a program to generate schematic diagrams of protein-ligand interactions. Protein Eng. 1995; 8:127–134. [PubMed: 7630882]

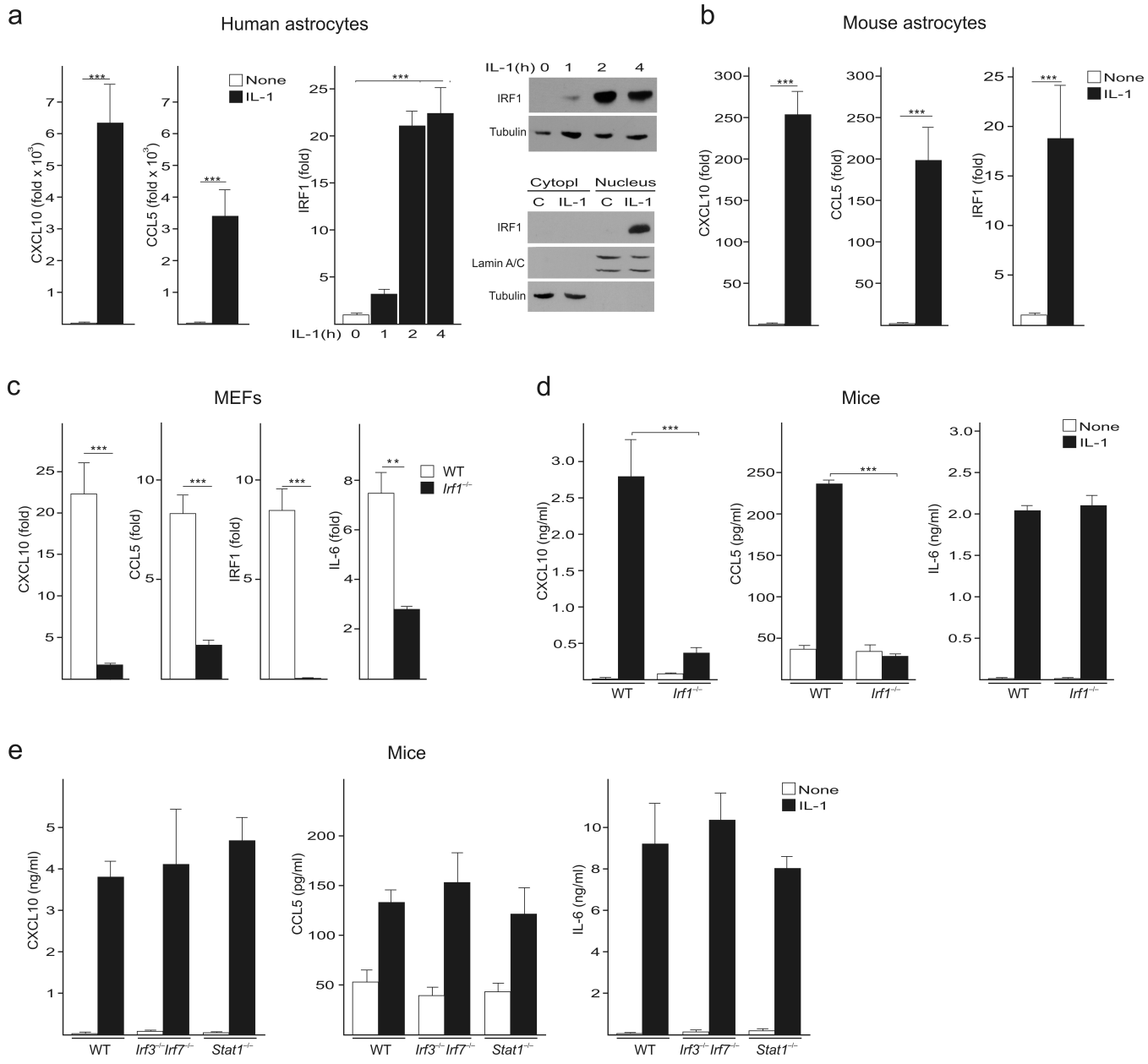

Figure 1. IRF1 is critical for IL-1-induced expression of CXCL10 and CCL5. (a) (Left panels) Primary human astrocytes were stimulated with IL-1 (10 ng/ml) for 8h or as indicated, and expression of *Cxcl10*, *Ccl5*, and *Irf1* mRNA was analyzed by TaqMan qPCR. Data are normalized to the expression of GAPDH mRNA and presented relative to the expression in untreated cells. **(Right panels)** Human astrocytes were treated with IL-1 for the indicated times and accumulation of IRF1 protein in total cell lysates (top) and in cytoplasmic and nuclear extracts (bottom) at 2h was analyzed by immunoblotting. Lamin A/C and tubulin were used as controls. **(b)** Primary mouse astrocytes were stimulated with IL-1 for 2h, **(c)** mouse embryonic fibroblasts (MEFs) from *Irf1*$^{-/-}$ mice and wild-type littermates were stimulated with IL-1 for 2h, and analyzed by Taq Man qPCR. (a-c) Error bars represent s.d. *** P<0.001, ** P<0.01. **(d)** Wild-type and *Irf1*$^{-/-}$ mice (n=3) and **(e)** *Irf3*$^{-/-}$*Irf7*$^{-/-}$, *Stat1*$^{-/-}$,

and wild-type mice (n=4) were injected i.p. with IL-1 (40 μg/kg). Blood was collected after 2h and serum concentrations of CXCL10, CCL5, and IL-6 were determined by ELISA. Error bars represent s.e.m. *** P<0.001, ** P<0.01.

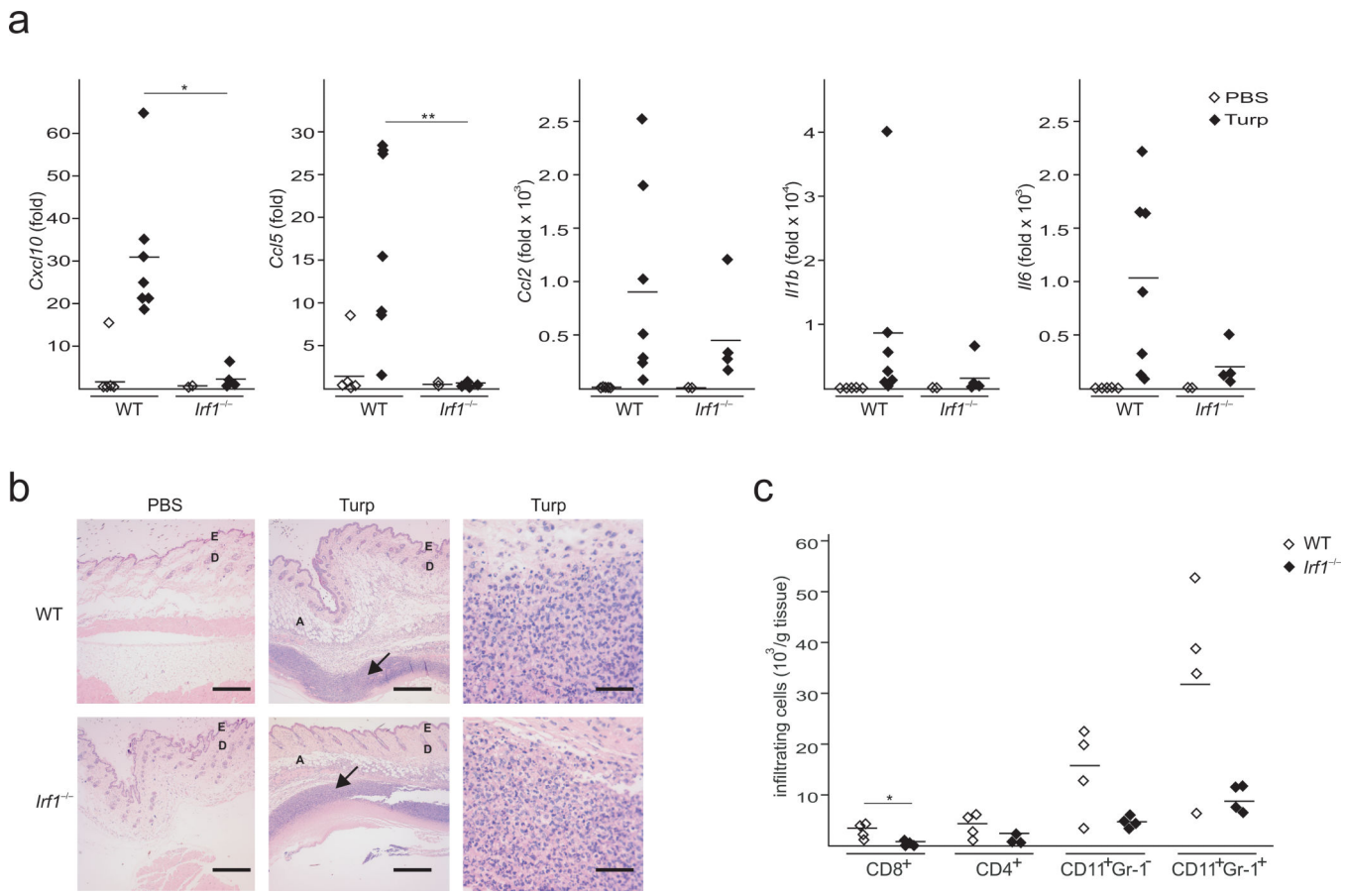

Figure 2. IRF1 is required for recruitment of mononuclear cells into sites of sterile inflammation

Irf1$^{-/-}$ mice or wild-type littermates were injected s.c. with 50 μl of PBS or turpentine (turp). Skin together with muscles at the sites of injection was collected after 8h **(a)** or 24h **(b, c)**. **(a)** Expression of *Cxcl10*, *Ccl5*, *Ccl2*, *Il1b* and *Il6* mRNA was analyzed by TaqMan qPCR. Error bars represent s.d. ** P<0.01, * P<0.05. **(b)** Tissues were stained with hematoxylin and eosin. Arrows indicate areas infiltrated by inflammatory cells; epidermis (E), dermis (D), and adipose tissue (A) are indicated. Bars represent 500 μm (central panels) or 50 μm (right panels). Data representative of two experiments.. **(c)** Cells were isolated from the infiltrated tissues and analyzed by flow cytometry. Data points in panels **a** and **c** represent individual mice with 4-7 mice per group. Error bars represent s.e.m. * P<0.05..

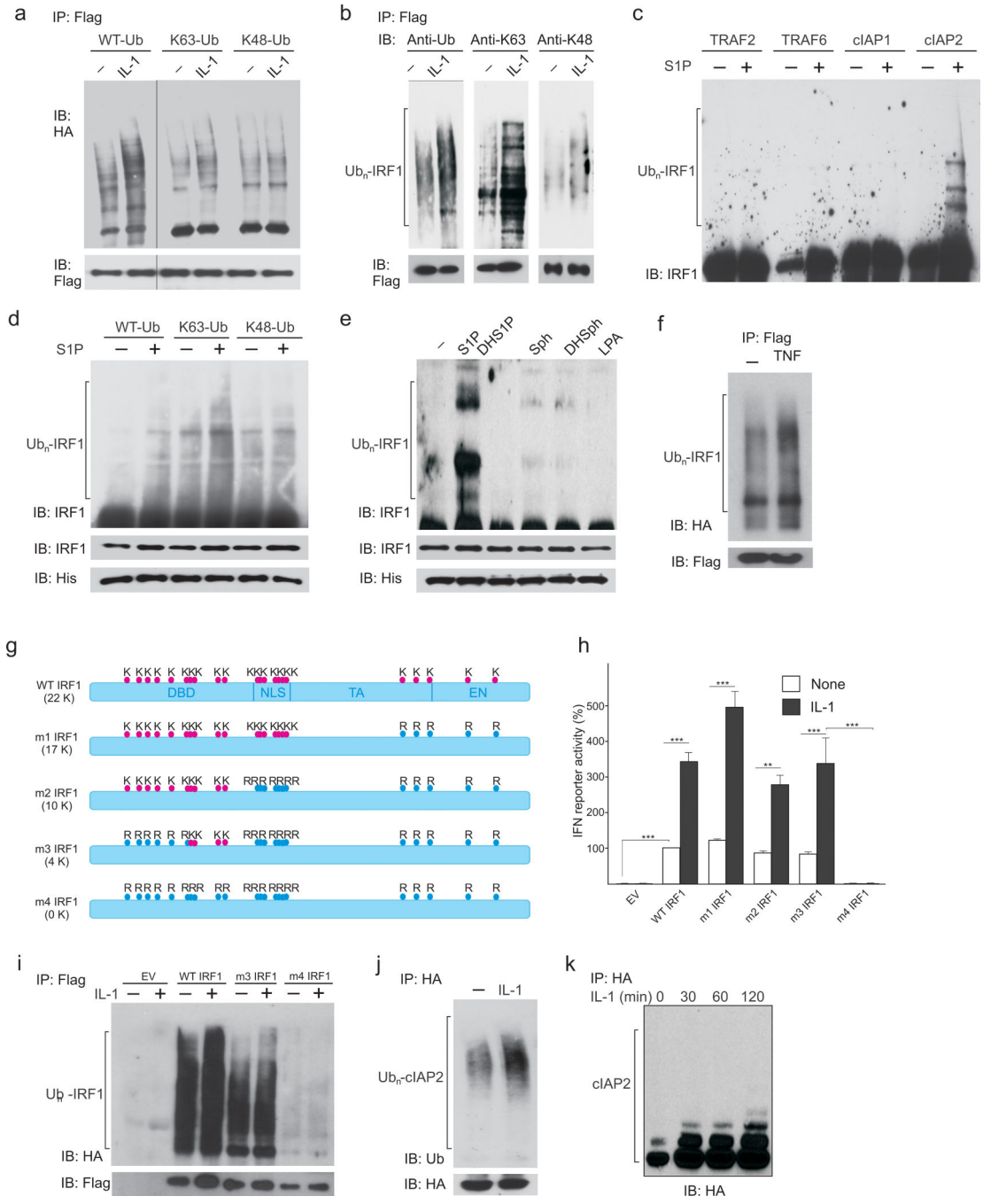

Figure 3. IL-1-induced K63-linked polyubiquitylation of IRF1 is mediated by cIAP2 in the presence of S1P

(a) HEK293 cells were transfected with expression plasmids encoding IRF1-FLAG, and HA-tagged wild-type- (WT-Ub), K63-only- (K63-Ub), or K48-only-ubiquitin (K48-Ub). 48 hours later, cells were stimulated with IL-1 for 2h, IRF1 was immunoprecipitated with anti-FLAG beads, and ubiquitylation was analyzed by immunoblotting using anti-HA antibodies. **(b)** HEK293 cells transfected with IRF1-FLAG were stimulated with IL-1 for 2 h, IRF1 was immunoprecipitated with anti-FLAG beads, and ubiquitylation was analyzed by

immunoblotting using anti-ubiquitin, anti-K63-ubiquitin or anti-K48-ubiquitin antibodies. **(c)** *In vitro* ubiquitylation assays were carried out with purified IRF1-FLAG, TRAF2, TRAF6, recombinant cIAP1 or cIAP2, ATP, E1, UbcH5a, and ubiquitin in the absence or presence of 100 nM S1P. Ubiquitylation was detected by immunoblotting using anti-IRF1 antibodies. **(d)** *In vitro* ubiquitylation was carried out with purified IRF1-FLAG, *E. coli* expressed cIAP2, ATP, E1, Ubc5a, and either wild type- (WT-Ub), K63-only- (K63-Ub), and K48-only-ubiquitin (K48-Ub) with/without 100 nM S1P. **(e)** *In vitro* ubiquitylation was analyzed in the absence or presence of 100 nM dihydro-S1P (DHS1P), S1P, sphingosine (Sph), dihydro-sphingosine (DHSph) or lysophosphatic acid (LPA). **(f)** HEK293 cells expressing IRF1FLAG and HA-tagged K63-Ub were stimulated with TNF for 2h, IRF1 was immunoprecipitated with anti-FLAG beads, and ubiquitylation was analyzed by immunoblotting using anti-HA antibodies. **(g)** Mouse IRF1 mutants: lysines (K), arginines (R), DNA binding domain (DBD), nuclear localization sequence (NLS), transactivation (TA) and enhancer (EN) domains are indicated. Numbers in parentheses indicate the number of lysine residues present. **(h)** HEK293 cells transfected with interferon-β (IFN) luciferase reporter, Renilla luciferase and IRF1 expression plasmids were stimulated with IL-1 for 6h. IFN reporter activities are shown relative to unstimulated cells expressing wild-type IRF1. Error bars represent s.d. *** $P<0.001$, ** $P<0.01$. **(i)** HEK293 cells expressing the indicated IRF1-FLAG proteins and HA-tagged K63-Ub were stimulated with IL-1 for 2h, IRF1 was immunoprecipitated with anti-FLAG beads, and IRF1 ubiquitylation was analyzed by immunoblotting using anti-HA antibodies. **(j)** HEK293 cells expressing cIAP2-HA were stimulated with IL-1 for 2h as indicated, cIAP2 was immunoprecipitated using anti-HA antibodies, and its ubiquitylation was analyzed by immunoblotting using anti-ubiquitin antibodies. **(k)** HEK293 cells expressing cIAP2-HA were stimulated with IL-1 as indicated, cIAP2 was immunoprecipitated using anti-HA antibodies, and analyzed by immunoblotting using anti-HA antibodies.

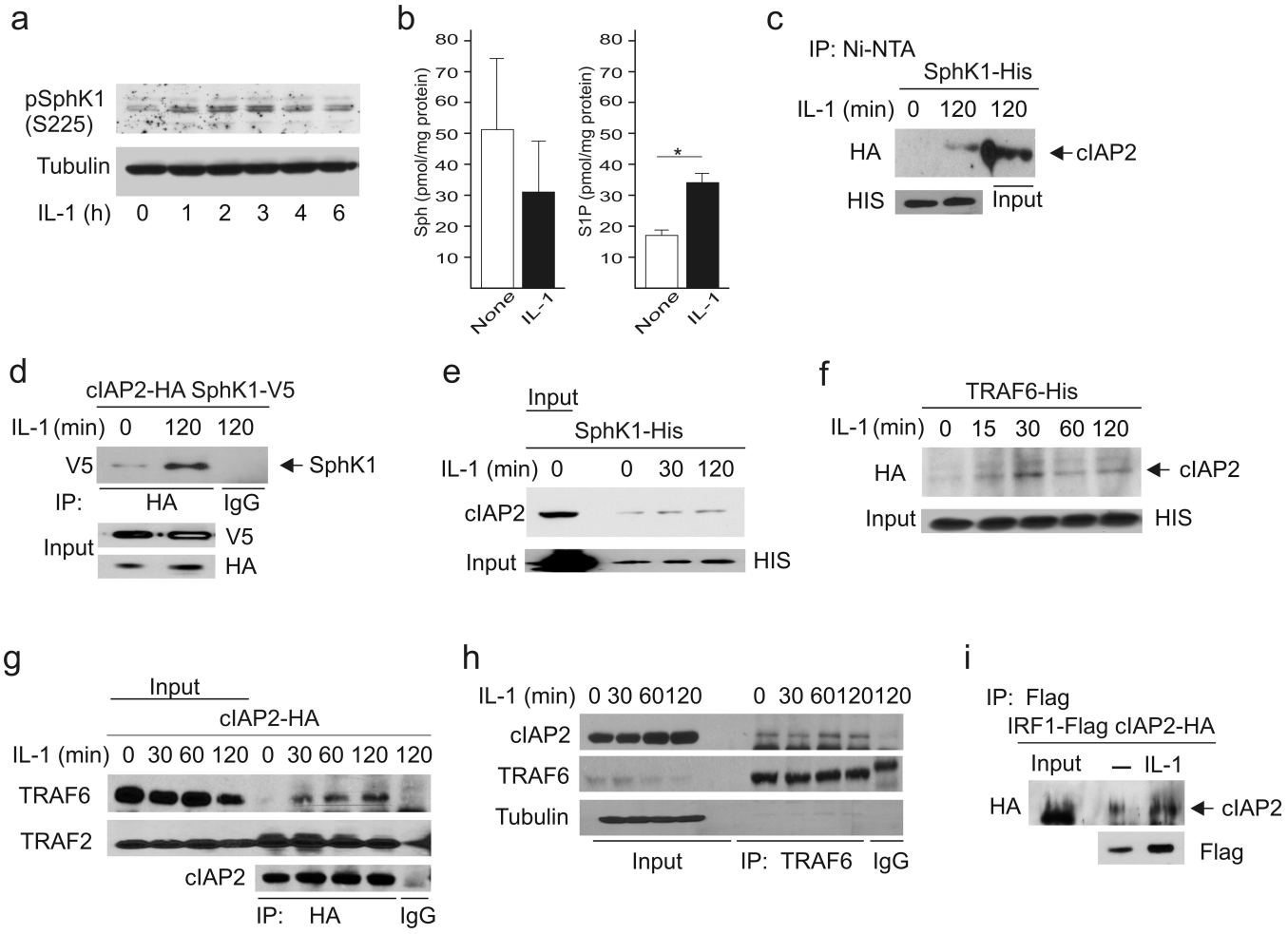

Figure 4. IL-1 induces formation of a TRAF6-cIAP2-SphK1 complex that also contains IRF1

(a) HEK293 cells were stimulated with IL-1 for the indicated times and phosphorylation of SphK1 was analyzed using anti-phospho-SphK1(Ser225) antibodies. **(b)** Astrocytes were stimulated with IL-1 for 2 h and Sph and S1P in medium were measured by LC-ESI-MS/MS. Error bars represent s.e.m. *, P = 0.075. **(c,d)** HEK293 cells were transfected with expression plasmids encoding SphK1-His and cIAP2-HA and stimulated with IL-1 as indicated. **(c)** SphK1-containing complexes were captured on Ni-NTA beads and cIAP2 was detected by immunoblotting using anti-HA antibodies. **(d)** Samples were immunoprecipitated with anti-HA antibodies or control IgG, and coimmunoprecipitated SphK1 was detected by immunoblotting using anti-V5 antibodies. **(e)** HEK293 cells were transfected with an expression plasmid encoding SphK1-His and stimulated with IL-1 as indicated. SphK1-containing complexes were captured on Ni-NTA beads, and endogenous cIAP2 was detected by immunoblotting using anti-cIAP2 antibodies. **(f)** HEK293 cells were transfected with expression plasmids encoding TRAF6-His and cIAP2-HA and stimulated with IL-1 as indicated. TRAF6-containing complexes were captured on Ni-NTA beads, and cIAP2 was detected by immunoblotting using anti-HA antibodies. **(g)** HEK293 cells expressing cIAP2-HA were stimulated with IL-1 as indicated. Samples were immunoprecipitated with anti-HA antibodies or control IgG, and coimmunoprecipitated

TRAF6 and TRAF2 were detected by immunoblotting. **(h)** HEK293 cells were stimulated with IL-1 as indicated. Samples were immunoprecipitated with anti-TRAF6 antibodies or control IgG, and coimmunoprecipitated cIAP2 was detected by immunoblotting. **(i)** HEK293 cells expressing IRF1-FLAG and cIAP2-HA were stimulated with IL-1 for 2h. IRF1 was immunoprecipitated with anti-FLAG beads, and cIAP2 was detected by immunoblotting using anti-HA antibodies.

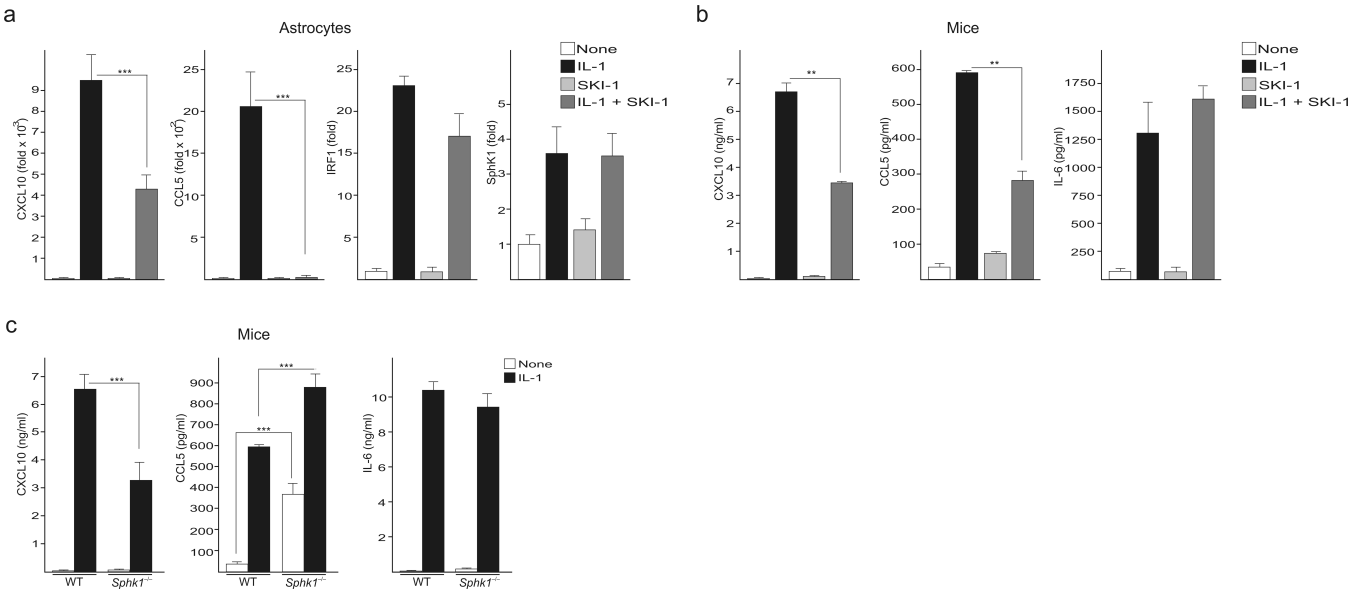

Figure 5. SphK1 activity is critical for activation of CXCL10 and CCL5 expression by IL-1

(a) Primary human astrocytes were pretreated with 5 μM SKI-1 for 30 min and then stimulated with IL-1 (10 ng/ml) for 8h. Expression of *Cxcl10*, *Ccl5*, *Irf1* and *Sphk1* mRNA was analyzed by TaqMan qPCR. Error bars represent s.d. *** P<0.001. **(b)** Wild-type mice (n=3) were injected i.p. with SK1-I (10 mg/kg). One-hour later mice were injected i.p. with IL-1 (40 μg/kg). Blood was collected after 2h and serum concentrations of CXCL10, CCL5, and IL-6 were determined by ELISA. **(c)** *Sphk1*$^{-/-}$ mice and wild-type littermates (n=3) were injected i.p. with IL-1 (40 μg/kg). Blood was collected after 2h and serum concentrations of CXCL10, CCL5, and IL-6 were determined by ELISA. (b-c) Error bars represent s.e.m. *** P<0.001, ** P<0.01.

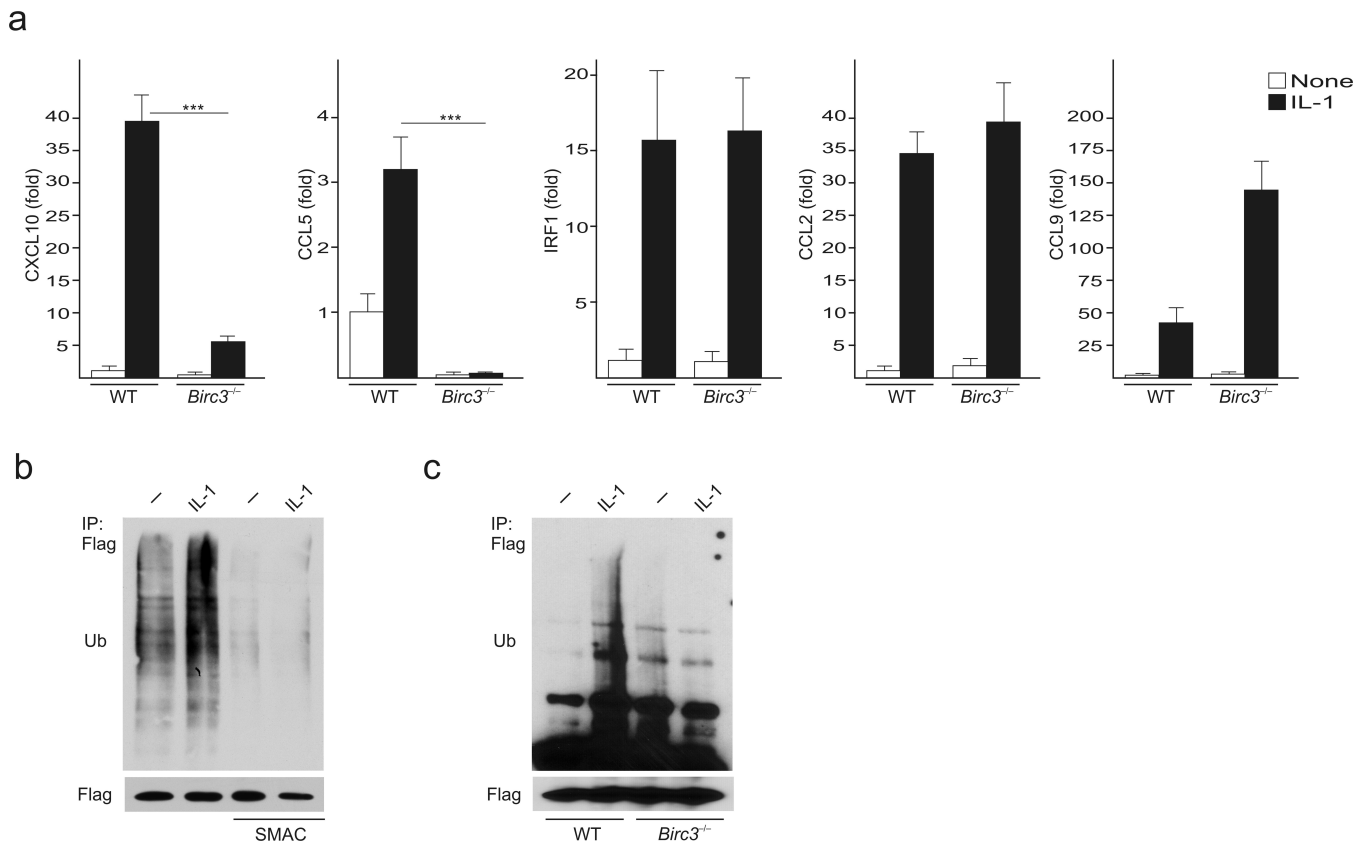

Figure 6. cIAP2 is required for IL-1-mediated upregulation of CXCL10 and CCL5 expression

(a) MEFs from *Birc3*$^{-/-}$ mice and wild-type littermates were stimulated with IL-1 for 8h, and expression of *Cxcl10*, *Ccl5*, *Ccl2*, *Cxcl9*, and *Irf1* mRNA was analyzed by TaqMan qPCR. Error bars represent s.d. *** P<0.001. **(b)** HEK293 cells expressing IRF1-FLAG were treated with 100 nM SMAC for 4h and then stimulated with IL-1 for 2h. IRF1 was immunoprecipitated with anti-FLAG beads, and ubiquitylation was analyzed by immunoblotting using anti-ubiquitin antibodies. **(c)** MEFs from *Birc3*$^{-/-}$ mice and wild-type littermates expressing IRF1-FLAG were stimulated with IL-1 for 2h. IRF1 was immunoprecipitated with anti-FLAG beads, and ubiquitylation was analyzed by immunoblotting using anti-ubiquitin antibodies.

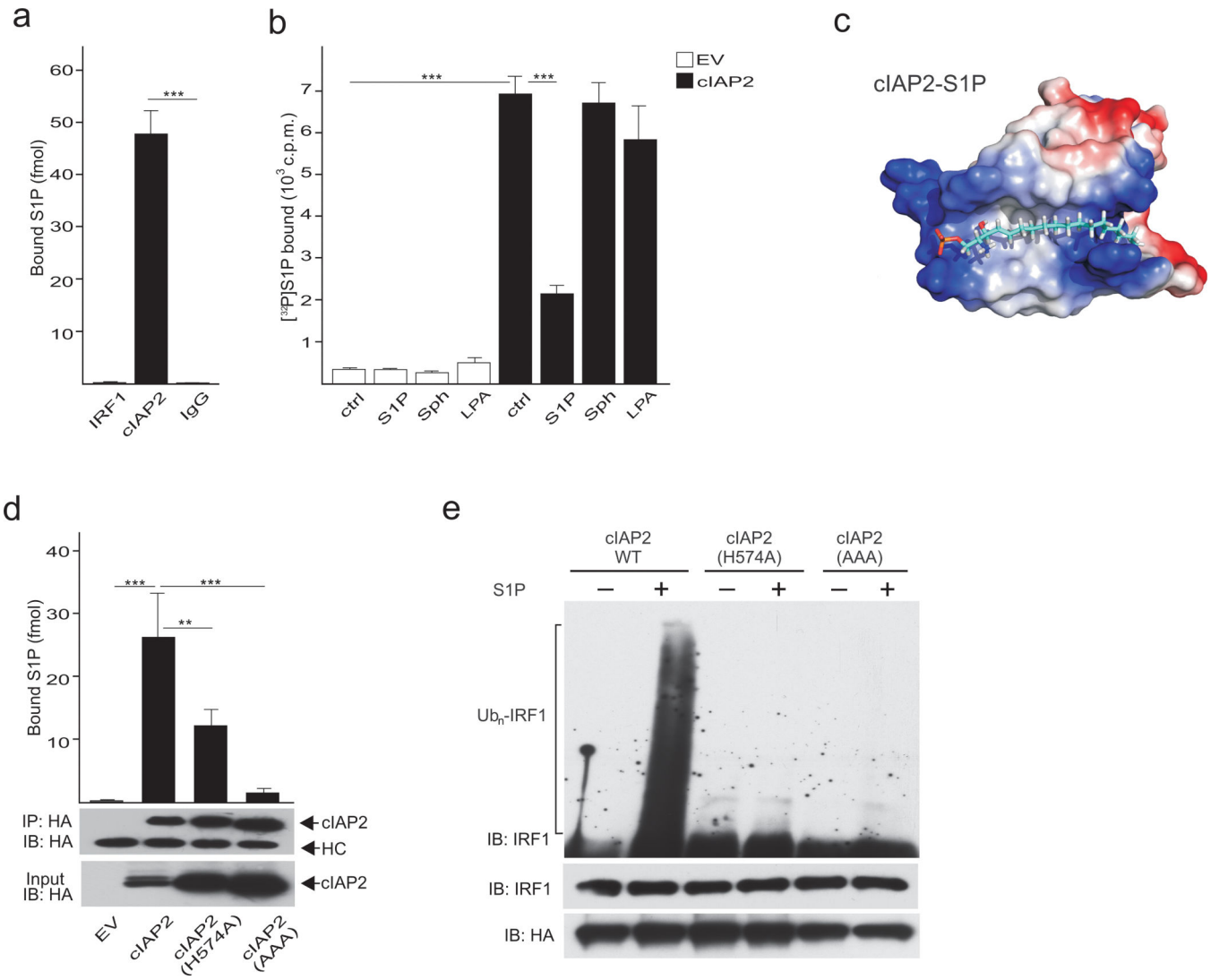

Figure. 7. S1P directly binds to cIAP2 and promotes IRF1 ubiquitylation

(a) Lysates of HEK293 cells expressing IRF1-FLAG or cIAP2-HA were immunoprecipitated with anti-FLAG, anti-HA antibodies or control IgG, and the amount of bound S1P was determined by LC-ESI-MS/MS. The data are averages of triplicate determinations and are expressed as femtomoles of S1P ± s.d. **(b)** Lysates from HEK293 cells expressing either cIAP2-HA or control vector were preincubated with 0.1 nM ^{32}P-labeled S1P and 1 μM unlabeled competitor (either S1P, DHS1P, Sph, or LPA) for 10 minutes. Lysates were immunoprecipitated with anti-HA agarose beads and binding of ^{32}P-labelled S1P was determined by scintillation counting. The data are averages ± s.d. **(c)** Docking of S1P into the pocket of the RING domain of cIAP2. Surface contour of the binding site with S1P was colored by electrostatic potential and figures were generated by Pymol. Estimated Ki values generated by AutoDock[45] for S1P and DHS1P are 3.72×10^{-6} and 19.72×10^{-6}, respectively. **(d)** Lysates from HEK293 expressing cIAP2-HA, cIAP2(H574A)-HA, cIAP2(AAA)-HA, or control vector were immunoprecipitated with anti-HA antibodies, and the amount of bound S1P was determined by LC-ESI-MS/MS. HC

indicates IgG heavy chain. (a-b, e) Error bars represent s.d. *** P<0.001, ** P<0.01. **(e)** *In vitro* ubiquitylation assays were carried out with purified IRF1-FLAG, cIAP2-HA, cIAP2(H574A)-HA, or cIAP2(AAA)-HA, and ATP, E1, UbcH5a, and ubiquitin in the absence or presence of 100 nM S1P. Ubiquitylation was detected by immunoblotting using anti-IRF1 antibodies.